World Journal of Radiology

Submit a Manuscript: http://www.wjgnet.com/esps/
Help Desk: http://www.wjgnet.com/esps/helpdesk.aspx
DOI: 10.4329/wjr.v8.i9.799

World J Radiol 2016 September 28; 8(9): 799-808
ISSN 1949-8470 (online)

MINIREVIEWS

Evaluation of DNA synthesis with carbon-11-labeled 4′-thiothymidine

Jun Toyohara

Jun Toyohara, Research Team for Neuroimaging, Tokyo Metropolitan Institute of Gerontology, Tokyo 173-0015, Japan

Author contributions: Toyohara J generated the figures and wrote the manuscript.

Supported by A Grant-in-Aid for Scientific Research from the Japan Society for the Promotion of Science, No. (B) 25293271.

Conflict-of-interest statement: The author declares that he has no competing interests.

Manuscript source: Invited manuscript

Correspondence to: Jun Toyohara, PhD, Theme Leader, Research Team for Neuroimaging, Tokyo Metropolitan Institute of Gerontology, 35-2 Sakae-cho, Itabashi-ku, Tokyo 173-0015, Japan. toyohara@pet.tmig.or.jp
Telephone: +81-3-39643210
Fax: +81-3-39641148

Received: February 25, 2016
Peer-review started: February 27, 2016
First decision: May 13, 2016
Revised: June 12, 2016
Accepted: July 29, 2016
Article in press: August 1, 2016
Published online: September 28, 2016

Abstract

In the cancer research field, the preferred method for evaluating the proliferative activity of cancer cells *in vivo* is to measure DNA synthesis rates. The cellular proliferation rate is one of the most important cancer characteristics, and represents the gold standard of pathological diagnosis. Positron emission tomography (PET) has been used to evaluate *in vivo* DNA synthetic activity through visualization of enhanced nucleoside metabolism. However, methods for the quantitative measurement of DNA synthesis rates have not been fully clarified. Several groups have been engaged in research on 4′-[methyl-^{11}C]-thiothymidine (^{11}C-4DST) in an effort to develop a PET tracer that allows quantitative measurement of *in vivo* DNA synthesis rates. This mini-review summarizes the results of recent studies of the *in vivo* measurement of cancer DNA synthesis rates using ^{11}C-4DST.

Key words: 4′-[methyl-^{11}C]-thiothymidine; DNA synthesis; Cell proliferation; Tumor; Positron emission tomography

Core tip: There is a continuous demand to measure *in situ* DNA synthesis rates in living human cancer. The thymidine derivative 4′-[methyl-^{11}C] thiothymidine (^{11}C-4DST) has the potential to visualize *in vivo* DNA synthesis rates with positron emission tomography (PET). To confirm whether ^{11}C-4DST is a valid DNA synthesis marker, clinical and basic research is being conducted at several PET centers in Japan, European Union, and the United States. This mini-review summarizes the progress of recent studies involving the *in vivo* imaging of cancer DNA synthesis using ^{11}C-4DST PET.

Toyohara J. Evaluation of DNA synthesis with carbon-11-labeled 4′-thiothymidine. *World J Radiol* 2016; 8(9): 799-808 Available from: URL: http://www.wjgnet.com/1949-8470/full/v8/i9/799.htm DOI: http://dx.doi.org/10.4329/wjr.v8.i9.799

INTRODUCTION

Rationale for DNA synthesis imaging

The basic principle of DNA synthesis measurement using positron emission tomography (PET) and the rationale for tracer development for DNA synthesis imaging were extensively reviewed by Bading *et al*[1], and Toyohara *et al*[2], respectively.

Briefly, thymidine is the only nucleoside that is exclusively incorporated into DNA. Therefore, DNA incorporation using [methyl-^{3}H]-thymidine is used as the gold standard for a cell proliferation marker. The challenge in visualizing *in vivo* DNA synthesis with ^{11}C-thymidine has been pursued since 1972[3]. Extensive developments in the 1990s and early 2000s realized the estimation of thymidine flux from blood to DNA in somatic and brain tumors[4-7]. From these studies, it became clear that the routine use of ^{11}C-thymidine has several limitations, including issues related to the use of radiolabeled catabolites, the short half-life of ^{11}C, and relatively difficult synthesis. While ^{11}C-thymidine is effectively incorporated into DNA, it is also rapidly catabolized by thymidine phosphorylase, which complicates image analysis. Thymidine is a substrate for mitochondrial thymidine kinase 2 as well as cytosolic thymidine kinase 1, which leads to the absence of cell proliferation related uptake in tissues with high mitochondria content, such as the heart. Therefore, the ideal tracer for DNA synthesis imaging requires resistance to catabolism by thymidine phosphorylase, selective phosphorylation by thymidine kinase 1, and ready incorporation into DNA (Figure 1).

4'-[methyl-^{11}C] thiothymidine

4′-[methyl-^{11}C] thiothymidine (^{11}C-4DST) is a derivative of thymidine in which the 4′-oxygen is replaced with sulfur and the 5-methyl group is radiolabeled with ^{11}C by the C-C cross-coupling reaction (Figure 2)[8,9]. The first synthesis conditions reported involved using 5-tributylstannyl-4′-thio-2′-deoxyuridine (precursor)/tris (dibenzylideneacetone) dipalladium (0) [$Pd_2(dba)_3$]/tri(*o*-tryl) phosphine [P(*o*-$CH_3C_6H_4)_3$] (1.5:1:3.9 in molar ratio) at 130 ℃ for 5 min in *N*,*N*-dimethylformamide (DMF), which gave the desired products at only 30% decay-corrected yields based on [^{11}C]CH_3I[9]. Subsequently, slight modifications of the conditions, using precursor/$Pd_2(dba)_3$/P(*o*-$CH_3C_6H_4)_3$/CuCl/K_2CO_3 (1.5:1:3.9:4:3.6) at 80 ℃, resulted in greatly improved decay-corrected yields (70%) based on [^{11}C]CH_3I[10]. Other reported conditions using precursor/$Pd_2(dba)_3$/P(*o*-$CH_3C_6H_4)_3$/CuCl/K_2CO_3 (25:1:32:2:5) at 80 ℃ also gave improved decay-corrected yields (42%-60%) using the two-pot method, and 65% by the one-pot method based on ^{11}C-CH_3I[11,12].

Preclinical evaluation indicated that the stability of ^{11}C-4DST within the body is higher than that of thymidine, and unlike 3′-deoxy-3′-[^{18}F]fluorothymidine (^{18}F-FLT), it is taken up into DNA as a substrate for DNA synthesis. Therefore, Toyohara *et al*[8,9] postulated that ^{11}C-4DST might be used as a valid *in vivo* DNA synthesis marker. ^{11}C-4DST was developed at the National Institute of Radiological Sciences (NIRS; Chiba, Japan) and has been approved for clinical use by the committee for medical use of cyclotron-produced radiopharmaceuticals of NIRS, as well as the medical use of cyclotron-produced radiopharmaceuticals and ethics committees of Tokyo Metropolitan Institute of Gerontology (TMIG; Tokyo, Japan). The first-in-human study was performed at TMIG in March 2010. ^{11}C-4DST was also described as ^{11}C-S-dThd[8,9], however, the names have since been unified to ^{11}C-4DST with the commencement of its clinical use[10].

INITIAL CLINICAL TRIAL

An initial clinical trial of ^{11}C-4DST, which was equivalent to a phase 1 trial, was performed according to guidelines approved in January 2008 by the institutional committee of TMIG for first-in-human use of novel radiopharmaceuticals. Briefly, five brain tumor patients volunteered to participate in a study of the side effects associated with administration of ^{11}C-4DST, which were assessed by clinical symptoms, physical findings, and blood tests. Concurrently, ^{11}C-4DST dynamic PET measurements were performed to assess the efficacy with which the desired function (DNA synthesis) can be measured. In addition, radiation dosimetry was estimated through whole-body PET measurement in three healthy volunteers.

The results of the initial clinical trial revealed no adverse events accompanying administration of ^{11}C-4-DST, and the effective dose was calculated as 4.2 μSv/MBq. Whole-body PET indicated ^{11}C-4DST accumulations in bone marrow and spleen, where DNA synthesis is active in the adult. These observations suggest that ^{11}C-4DST uptake reflects the dynamics of DNA synthesis activity (Figure 3). In addition, physiological accumulation of radioactivity was observed in the liver, kidney, and salivary glands, which are components of the metabolic excretion pathway. The levels of ^{11}C-4DST accumulation in the mediastinum, cerebral parenchyma, lungs, cardiac muscles, and skeletal muscles were very low.

The distribution of ^{11}C-4DST within the human body was different from that in rodents, and a high level of ^{11}C-4DST accumulation was observed in the human liver. This may have been due to species differences in ^{11}C-4DST metabolism; the metabolism of ^{11}C-4DST in humans is faster than that in rodents and produces hydrophilic metabolites. Treatment of the main component of the hydrophilic metabolites with β-glucuronidase results in the formation of ^{11}C-4DST. Therefore, the high level of ^{11}C-4DST accumulation in the human liver is due to conjugation of ^{11}C-4DST.

^{11}C-4DST is a nucleoside derivative and therefore does not readily pass through the blood-brain barrier. Thus, accumulation of radioactivity in normal brain is low. However, the majority of brain tumor lesions could be imaged, and the accumulation of ^{11}C-4DST in brain

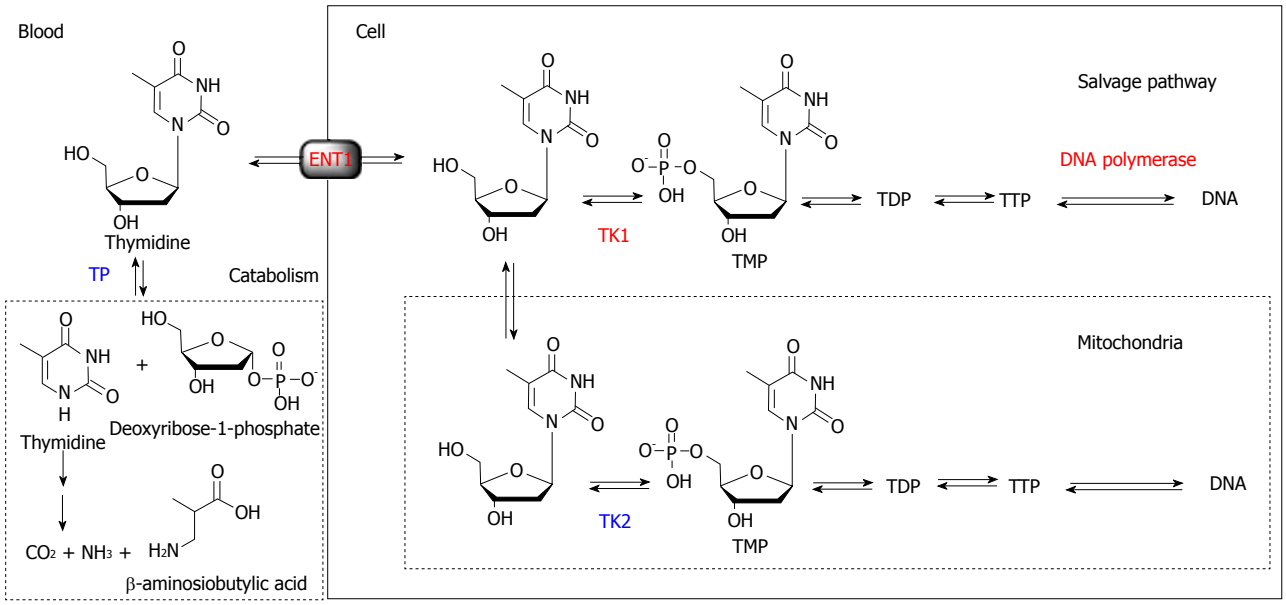

Figure 1 Rationale for designing an ideal DNA synthesis tracer for cell proliferation imaging. The ideal tracer must block catabolism by thymidine phosphorylase, while retaining anabolism by the salvage pathway. ENT1: Equilibrative nucleoside transporter 1; TDP: Thymidine di-phosphate; TMP: Thymidine monophosphate; TTP: Thymidine tri-phosphate; TK1: Thymidine kinase 1; TK2: Thymidine kinase 2; TP: Thymidine phosphorylase.

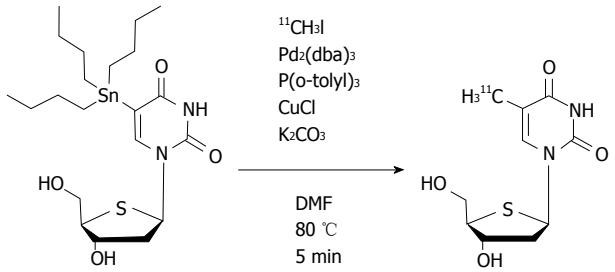

Figure 2 Radiosynthesis of 4'-[methyl-^{11}C]-thiothymidine. The imaging agent ^{11}C-4DST was synthesized by methylation of 5-tributylstannyl-4'-thio-2'-deoxyuridine *via* a palladium-mediated Stille cross-coupling reaction with ^{11}C-methyl iodide. ^{11}C-4DST: 4'-[methyl-^{11}C]-thiothymidine; DMF: N,N-Dimethylformamide; $P(o\text{-}tolyl)_3$: Tri(o-tryl)phosphine; $Pd_2(dba)_3$: Tris(dibenzylide neacetone)dipalladium(0).

tumor lesions varied depending on the treatment conditions. In some cases, the accumulation of ^{11}C-4DST was clearly different from ^{11}C-methionine (^{11}C-MET) images acquired at the same time. The images in Figure 4A shows a case that was resistant to the anticancer agent temozolomide, while the Figure 4B shows a case that was responsive to temozolomide. As can be seen in this figure, ^{11}C-4DST sensitively captures the responsiveness of the tumor cells toward radiotherapy or chemotherapy.

KINETIC ANALYSIS

Time-activity curves (TACs) of ^{11}C-4DST accumulation in brain tumors indicated irreversible kinetics, suggesting that ^{11}C-4DST might be metabolically trapped. In addition, Patlak graph analysis showed a linear plot, which supports the above suggestion[8,9]. The results of the preliminary kinetic analysis indicated that ^{11}C-4DST was irreversibly taken up into the DNA because ^{11}C-4DST fits the two-tissue three-compartment model, and k_4 is negligibly small. The value of k_3 (k_4 = 0) obtained by the analysis showed a strong correlation with K_i (k_4 = 0), which reflects the rate of ^{11}C-4DST incorporation flux (Pearson's r = 0.925, P = 0.001), and no correlation was observed with K_1 (k_4 = 0), which reflects intracellular transport. In addition, the standardized uptake value (SUV) showed the best correlation with K_i (Patlak) and also showed good correlations with K_i (k_4 = 0) and k_3 (k_4 = 0) (Pearson's r = 0.942, P = 0.0005; r = 0.857, P = 0.0065, respectively). The above results suggest that images of DNA synthesis might be obtained through non-quantitative analysis using SUV images.

In addition, we performed a basic validation study of ^{11}C-4DST accumulation kinetics into the DNA. The time course of the DNA uptake ratio in proliferating tissues in rats was illustrated by a Michaelis-Menten-type hyperbolic curve, and 50% of the radioactivity was taken into DNA at 5 and 8 min after administration in the duodenum and spleen, with maximum uptake ratios of 99% and 94%, respectively. The TACs of these tissues as a whole were almost identical to the TACs of DNA incorporated radioactivity (DNA fraction) and were different from the soluble non-DNA fraction (unchanged form + phosphorylated form) (Figure 5). On the other hand, in the AH109A rat liver cancer transplantation model, significant variation in DNA uptake rates between sampling sites was due to heterogeneity in the tumor tissues, with some regions exhibiting 60% DNA uptake at 1 min after administration (where cell proliferation is active). The above results indicate that the process of DNA uptake is the rate-limiting step in ^{11}C-4DST accumulation.

Furthermore, Plotnik *et al*[13] evaluated the kinetics of ^{3}H-4DST transport and metabolism in the human

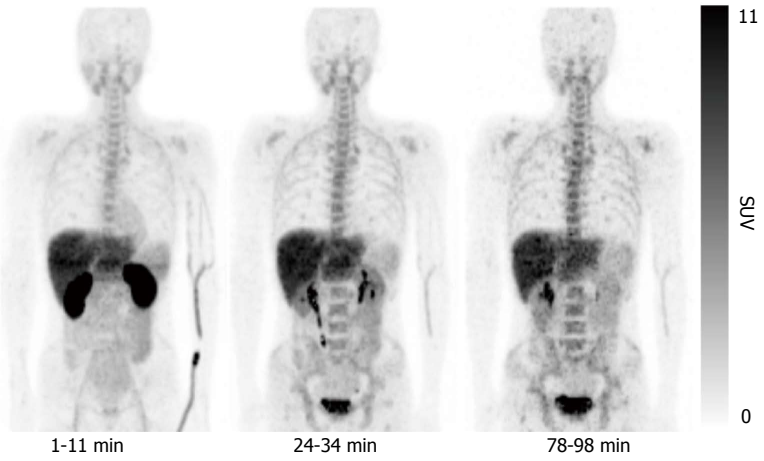

Figure 3 Representative whole-body decay-corrected maximum intensity-projection images of 4'-[methyl-^{11}C]-thiothymidine positron emission tomography images. ^{11}C-4DST showed high uptake in the excretory organs, such as the kidneys, liver, and urinary bladder. Moderate uptake was observed in the proliferative organs, such as bone marrow, spleen, and small intestine. The lowest uptake was observed in the non-proliferating tissues, such as muscle and lungs. This research was originally published in JNM[10]. ^{11}C-4DST: 4'-[methyl-^{11}C]-thiothymidine; SUV: Standardized uptake value.

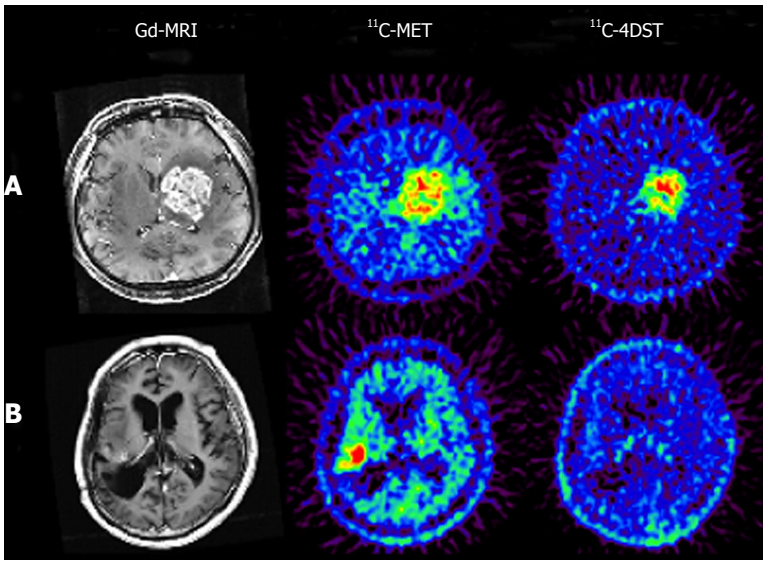

Figure 4 Brain tumor imaging in temozolomide-resistant (A) and -responsive (B) patients. DNA synthesis images provide completely different information from those obtained with an amino acid transport agent. In the case of recurrent anaplastic oligodendroglioma (A), both ^{11}C-MET and ^{11}C-4DST showed high uptake in the gadolinium-enhanced region of the MRI. However, the distribution pattern of each tracer in the tumor region was not identical. The tumor in this patient showed progressive enlargement despite continuous treatment with the DNA alkylating agent temozolomide. In the case of recurrent anaplastic astrocytoma (B), the patient received one course of treatment with temozolomide 3 d before PET examinations, and it was found that the ^{11}C-4DST uptake was negligible in the gadolinium-enhanced region where high uptake of ^{11}C-MET was observed. The enhanced tumor mass in this patient remained unchanged over 6 mo after commencement of temozolomide treatment. These observations suggest that DNA synthesis in the tumor was suspended by temozolomide treatment. Reprinted from Nariai *et al*[14], with the permission of Springer. ^{11}C-4DST: 4'-[methyl-^{11}C]-thiothymidine; ^{11}C-MET: ^{11}C-Methionine; Gd-MRI: Gadolinium-enhanced magnetic resonance image; PET: Positron emission tomography.

adenocarcinoma cell line A549 under exponential-growth conditions. ^{3}H-4DST behaved qualitatively similar to endogenous thymidine in terms of equilibrative nucleoside transporter dependent cellular transport, shapes of cellular uptake curves, and relative DNA incorporation levels. As 4DST closely mimics thymidine metabolism, ^{11}C-4DST should provide a robust measurement of DNA synthesis. However, overall ^{3}H-4DST metabolism was significantly lower than that of thymidine, which may reflect its lower affinity toward thymidine kinase 1. This slower metabolism might limit its usefulness because of the relatively short half-life of the ^{11}C label, especially in the case of slow-growing tumors like prostate cancer.

CLINICAL STUDY IN VARIOUS TUMOR TYPES

Although the presence of metabolites in blood was not desirable in terms of quantitative measurement, the results of the ^{11}C-4DST early clinical trials indicated that its usability exceeded the drawbacks. In addition, as

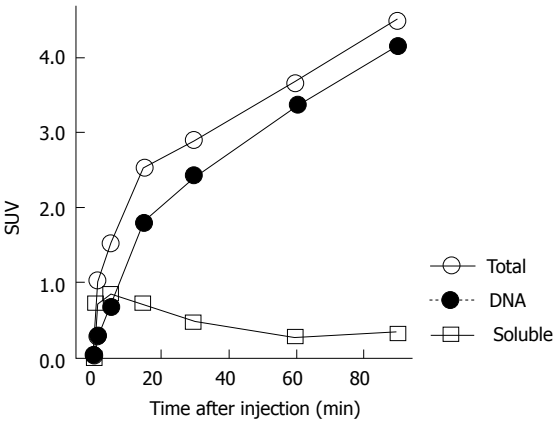

Figure 5 Time courses of 4'-[methyl-^{11}C]-thiothymidine activity in the mouse duodenum. The data is presented as the SUVmean in the indicated fractions (n = 3-5). Rapid DNA separation was performed using the DNAzol reagent[30]. The increase in total tissue radioactivity paralleled that of DNA incorporated radioactivity. The soluble fraction (4DST itself, phosphorylated 4DST, and other metabolites) was low and stable at 30 min after tracer injection. The contribution of the DNA incorporation process overshadows both the phosphorylation and dephosphorylation rates at later phases of the PET scan. PET: Positron emission tomography; SUV: Standardized uptake value.

high usability of ^{11}C-4DST was expected from the basic data obtained in animal experiments[8,9], collaborative research was initiated with the National Center for Global Health and Medicine (NCGM; Tokyo, Japan) and Kagawa University (Kagawa, Japan). In this collaborative research, technology transfer of radiosynthesis was first performed and then an application was submitted to the ethics committee. The clinical trial was started at approximately the same time as the early clinical trial performed at TMIG. A study to fundamentally support the clinical data is also being conducted in collaboration with the University of Groningen Medical Center (UMCG; Groningen, The Netherlands) and the University of Washington (Seattle, WA).

BRAIN TUMORS

Initial clinical studies of ^{11}C-4DST in brain tumors were performed at TMIG[14]. Fourteen patients with brain tumors (11 malignant gliomas, 2 metastatic tumors, 1 craniopharyngioma, and 1 malignant lymphoma) were included and the uptake of ^{11}C-4DST and ^{11}C-MET into gadolinium-enhanced lesions on T1 weighted magnetic resonance image (MRI) was evaluated. In this study, Nariai *et al*[14] observed a unique characteristic of ^{11}C-4DST in one case. They observed a marked decrease of ^{11}C-4DST uptake into metastatic lung cancer 5 d after gamma knife therapy. Although ring form enhancement with cystic formation did not disappear completely, tumor growth ceased with this treatment and the patient has maintained favorable activity of daily living 1 year after treatment (Figure 6). In another case, ^{11}C-4DST could differentiate oligodendroglioma from malignant transformation (Figure 7). However, ^{11}C-MET showed increased uptake, which indicates malignant transformation. An increased microvessel surface of

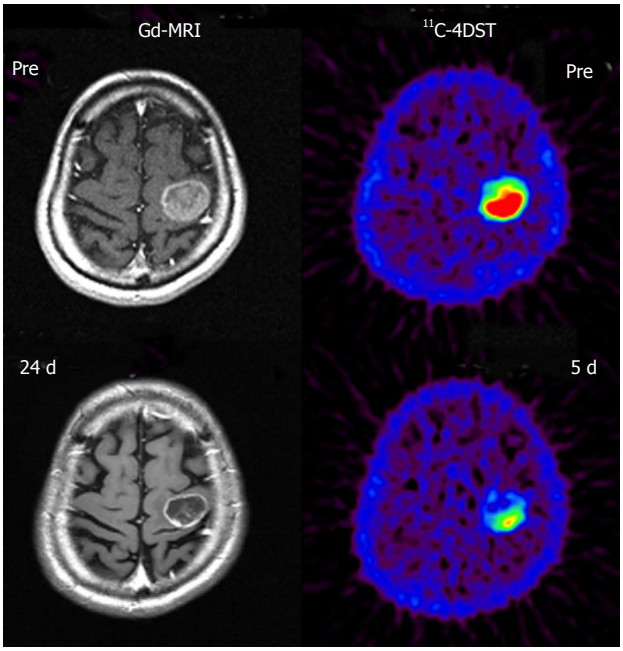

Figure 6 Early evaluation of the effectiveness of radiosurgery with 4'-[methyl-^{11}C]-thiothymidine positron emission tomography. A marked decrease in ^{11}C-4DST uptake into metastatic lung cancer was observed 5 d after gamma knife radiosurgery. Although ring form enhancement with cystic formation did not disappear completely, tumor growth was halted by this treatment and the patient has maintained favorable activity of daily living 1 year after treatment. These observations indicated that the effectiveness of gamma knife therapy was correctly monitored by ^{11}C-4DST only 5 d after treatment. Reprinted from Nariai *et al*[14], with the permission of Springer. ^{11}C-4DST: 4'-[methyl-^{11}C]-thiothymidine; Gd-MRI: Gadolinium-enhanced magnetic resonance image.

oligodendroglioma causes the increased uptake of ^{11}C-MET despite low proliferation of the tumor cells. This case study suggests that ^{11}C-4DST accumulates in growing tumors but not in tumors stabilized by treatment. ^{11}C-4DST uptake into tumors was not influenced by increased transport from blood to tissue, as observed for ^{11}C-MET.

Further in-depth research of ^{11}C-4DST in brain tumors was conducted at Kagawa University. Toyota *et al*[15] directly compared ^{11}C-4DST and ^{18}F-FLT in the same subjects. Twenty patients with primary (n = 9) and recurrent (n = 11) gliomas underwent ^{11}C-4DST and ^{18}F-FLT PET/CT scans. In the normal brain, ^{11}C-4DST uptake was significantly higher than ^{18}F-FLT (SUVmean; 0.34 ± 0.06 *vs* 0.19 ± 0.04, P < 0.001 by paired t-test). Individual ^{11}C-4DST SUVmax in the tumor was very similar to ^{18}F-FLT. Therefore, the average tumor-to-normal tissue uptake (T/N) ratio of ^{18}F-FLT in the tumor was significantly higher than that of ^{11}C-4DST (10.55 ± 5.45 *vs* 5.96 ± 3.86, P < 0.001 by paired t test), resulting in better tumor visualization with ^{18}F-FLT. Both of these tracers did not show significant differences in T/N ratio among different glioma grades. Linear regression analysis showed a significant correlation between proliferative activity indicated by the Ki-67 labeling index and the T/N ratios of ^{11}C-4DST (r = 0.50, P < 0.05) and ^{18}F-FLT (r = 0.55,

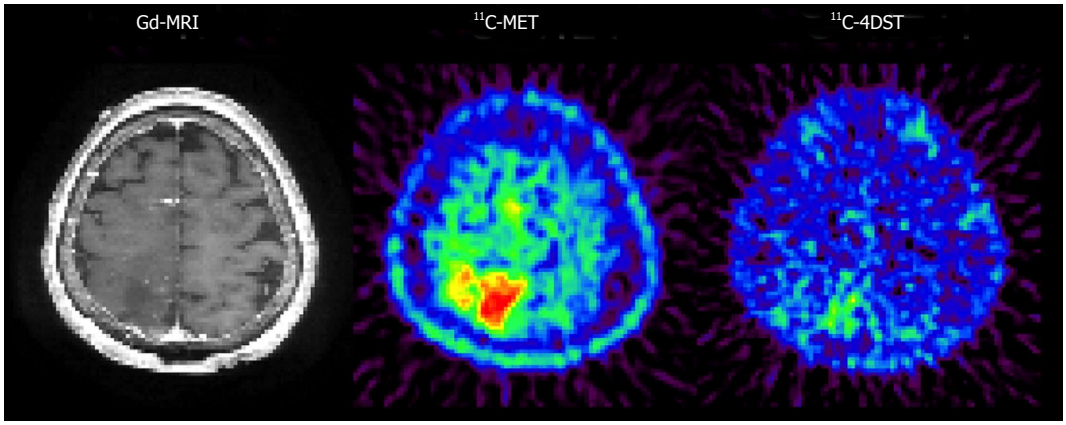

Figure 7 4'-[methyl-^{11}C]-thiothymidine uptake in oligodendroglioma. A patient was diagnosed with grade 2 astrocytoma during the initial operation. At the 1-year follow-up, an enhanced lesion appeared on MRI and ^{11}C-MET uptake increased around the initially resected lesion. These findings suggested that the malignant transformation of astrocytoma occurred. However, ^{11}C-4DST uptake into the tumor was not different from basal brain levels. The pathological diagnosis at the second operation was grade 2 oligodendrocytoma with a newly appearing oligodendroglioma component, but without malignant transformation. Reprinted from Nariai *et al*[14], with the permission of Springer. ^{11}C-4DST: 4'-[methyl-^{11}C]-thiothymidine; ^{11}C-MET: ^{11}C-Methionine; Gd-MRI: Gadolinium-enhanced magnetic resonance image.

$P < 0.05$). A highly significant correlation was observed between the individual T/N ratios of ^{11}C-4DST and ^{18}F-FLT ($r = 0.79$, $P = 0.0001$). These results indicate that the uptake pattern and uptake values of ^{11}C-4DST in gliomas are similar to those of ^{18}F-FLT. Two exceptions were observed, one non-enhanced primary diffuse astrocytoma and one recurrent glioblastoma with an oligodendroglioma component, in which only ^{18}F-FLT could detect the tumor well, with ^{11}C-4DST showing no and faint uptake in the tumor, respectively.

In a follow-up study, Tanaka *et al*[16] retrospectively evaluated ^{11}C-4DST uptake in 23 patients with newly diagnosed gliomas, and correlated the results with the Ki-67 index and tumor grade in comparison with ^{11}C-MET[16]. ^{11}C-4DST PET/CT showed a slightly lower detection rate for gliomas than ^{11}C-MET (87% *vs* 96%); however, the difference was not statistically significant. The tracer uptake for normal brain tissue of ^{11}C-4DST was significantly lower than that of ^{11}C-MET (0.48 ± 0.19 *vs* 1.52 ± 0.36, $P < 0.001$). The tracer uptake of ^{11}C-4DST in the tumor was also significantly lower than that of ^{11}C-MET (2.14 ± 1.58 *vs* 5.39 ± 2.22, $P < 0.001$). Therefore, no significant difference in T/N ratio or metabolic tumor volume (MTV: volume with a threshold of 40% of SUVmax) was observed between ^{11}C-4DST and ^{11}C-MET. A weak correlation was observed between ^{11}C-4DST and Ki-67 index for SUVmax ($r = 0.46$, $P < 0.03$), for T/N ratio ($r = 0.43$, $P < 0.05$), and for MTV ($r = 0.68$, $P < 0.001$) and between ^{11}C-MET MTV and Ki-67 index ($r = 0.43$, $P < 0.04$). Among them, the correlation coefficient between ^{11}C-4DST MTV and Ki-67 index was the highest. There was a significant difference in SUVmax of ^{11}C-4DST between grades Ⅱ and Ⅳ ($P < 0.03$) and in MTV between grades Ⅱ and Ⅳ ($P < 0.0009$) and grades Ⅲ and Ⅳ ($P < 0.02$).

HEAD AND NECK CANCER

Ito *et al*[17] prospectively compared the diagnostic value of ^{11}C-4DST PET/CT and ^{18}F-FDG PET/CT in patients with head and neck squamous cell carcinoma (HNSCC)[17]. Thirty-eight patients with advanced HNSCC underwent ^{11}C-4DST PET/CT and ^{18}F-FDG PET/CT before treatment. All patients were followed for 13.5 ± 7.5 mo to monitor recurrence. The total lesion glycolysis (TLG) for ^{18}F-FDG and total lesion proliferation (TLP) for ^{11}C-4DST were used as outcome measures of the combination of functional information and volumetric data to predict patient prognosis[18-21]. Nine of the 38 patients with post-treatment recurrence were identified. Receiver operating characteristic curves for $TLG_{3.0}$ (sensitivity: 89%; specificity: 72%) and $TLP_{2.5}$ (sensitivity: 89%; specificity: 55%) showed the highest prognostic ability for recurrence. There was no significant correlation between the Ki-67 index and whether ^{18}F-FDG SUVmax ($P = 0.81$) or ^{11}C-4DST SUVmax ($P = 0.49$) was observed in the primary tumor. One possible reason for this finding may be that the Ki-67 index was obtained mainly from biopsy specimens, not from resected specimens.

LUNG CANCER

At NCGM, the first study focused mainly on lung cancer cases[22]. The subjects were 18 primary lung cancer patients (19 lesions) who underwent segmental resection and lymph node dissection. ^{18}F-FDG PET/CT and ^{11}C-4DST PET/CT were performed in these patients during the same period and SUVmax was measured at the lesioned region in each patient. The results and histopathological evaluation (*e.g.*, Ki-67 index) were compared. The observed histological types included 16 adenocarcinomas (including bronchioloalveolar carcinoma), 2 squamous cell carcinomas, and 1 large cell carcinoma, and the average tumor size was 27.2 mm. The average levels of SUVmax in the primary tumors were 2.9 ± 1.0 and 6.2 ± 4.5 for ^{11}C-4DST and ^{18}F-FDG, respectively; SUVmax of ^{11}C-4DST was

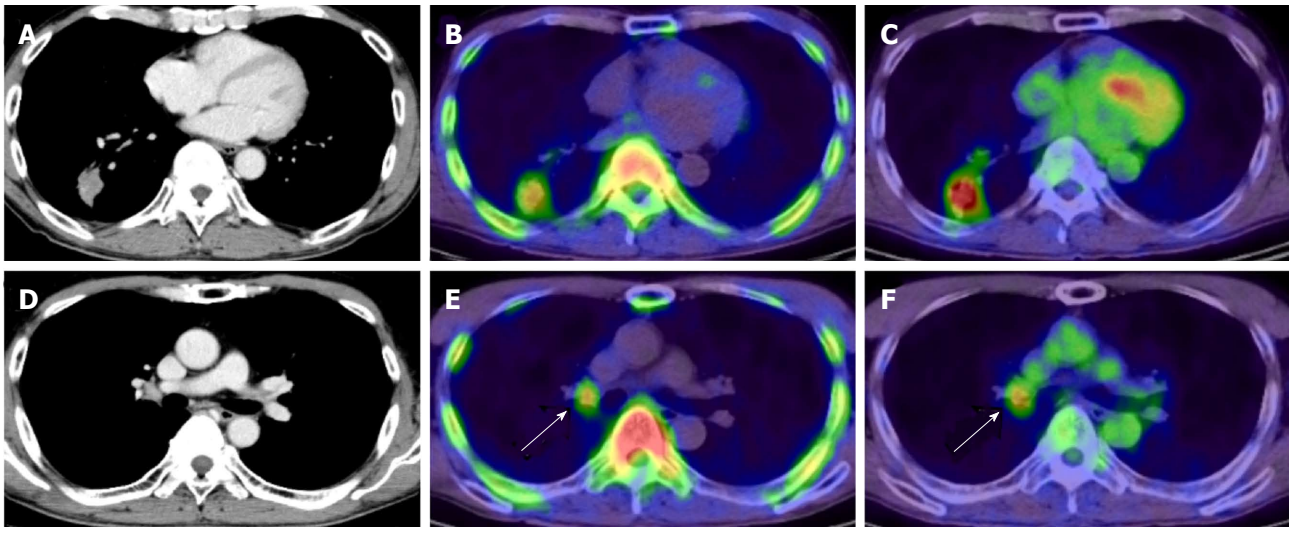

Figure 8 4'-[methyl-^{11}C]-thiothymidine images in non-small cell lung cancer. Axial images of CT (A), ^{11}C-4DST PET (B), and ^{18}F-FDG PET (C) in a 58-year-old man with lung adenocarcinoma in the right lower lobe. Radioactivity of ^{11}C-4DST in the ascending aorta (representing blood pool) is lower than that of ^{18}F-FDG. Both ^{11}C-4DST and ^{18}F-FDG clearly visualize lung lesions. Right hilar lymph node metastasis is confirmed on CT (D), and uptake of both ^{11}C-4DST PET (E) and ^{18}F-FDG PET (F) identifies the lesion (arrow). However, ^{11}C-4DST images are clearer than ^{18}F-FDG images because of low physiologic ^{11}C-4DST in the mediastinum (blood pool). This research was originally published in JNM[22]. ^{11}C-4DST: 4'-[methyl-^{11}C]-thiothymidine; PET: Positron emission tomography; ^{18}F-FDG: 2-Deoxy-2-[^{18}F]fluoro-D-glucose; CT: Computed tomography.

approximately half that of ^{18}F-FDG. Figure 8 shows representative images of ^{11}C-4DST in patients with lung adenocarcinoma. ^{11}C-4DST clearly visualized hilar lymph node metastasis because of low physiologic accumulation in the mediastinum blood pool. The correlation coefficients between SUVmax and Ki-67 index were 0.81 and 0.71 for ^{11}C-4DST and ^{18}F-FDG, respectively, and that of ^{11}C-4DST was significantly higher. ^{11}C-4DST appears to be effective as a PET tracer in primary lung cancer indicating DNA synthetic activity (cell proliferation activity).

The diagnostic ability of ^{11}C-4DST for detecting regional lymph node metastasis of non-small cell lung cancer (NSCLC) was prospectively evaluated by the same group (NCGM)[23]. A total of 31 patients with NSCLC underwent ^{11}C-4DST PET/CT and ^{18}F-FDG PET/CT. Patients were followed for up to 2 years to assess disease-free survival. A total of 123 nodal groups were defined for 27 patients, with proven malignancy in 17 nodal groups of 9 patients. The sensitivity on a per-node basis was significantly higher with ^{11}C-4DST than with ^{18}F-FDG (82.5% *vs* 29.4%, $P < 0.002$). In contrast, the specificity on a per-node basis was significantly lower with ^{11}C-4DST than with ^{18}F-FDG (71.7% *vs* 85.8%, $P < 0.02$). The disease-free survival rate with positive ^{11}C-4DST uptake in nodal lesions was 0.35, which was considerably lower than the rate of 0.83 with negative findings ($P = 0.04$). Interestingly, nodal staging by ^{11}C-4DST was the most influential prognostic factor ($P = 0.05$) among the factors tested. The high sensitivity of ^{11}C-4DST for nodal metastasis indicates that it may be efficient in detecting lymph node micrometastasis.

MULTIPLE MYELOMA

In whole-body imaging diagnosis of multiple myeloma (MM), it was demonstrated that myeloma has various characteristics that become prominent at different stages, including energy metabolism (^{18}F-FDG), production of M protein (^{11}C-MET), and cell proliferation (^{11}C-4DST). We hope to be able to accurately determine the periods where follow-up observation is sufficient and aggressive chemotherapy is necessary, to optimize treatment in such cases. Okasaki *et al*[24] prospectively evaluated the possibility of ^{11}C-MET and ^{11}C-4DST whole-body PET/CT when searching for bone marrow involvement in patients with MM, in comparison with those for ^{18}F-FDG PET/CT and aspiration cytology[24]. A total of 64 patients with MM or monoclonal gammopathy of undetermined significance (MUGS) underwent three whole-body PET/CT scans with ^{18}F-FDG, ^{11}C-MET, and ^{11}C-4DST within a period of 1 wk. The tracer accumulation was evaluated as positive, equivocal, or negative for 55 lytic lesions visualized using CT in 24 patients. To verify tracer uptake by lesions, 36 patients underwent bone aspiration cytology within 1 wk of the three PET/CT scans. The SUVmax of ^{11}C-4DST in lytic lesions were highest among the three tracers. ^{11}C-4DST and ^{11}C-MET provided clearer findings than ^{18}F-FDG for lytic lesions. A typical MM patient with multiple active lesions is shown in Figure 9. ^{11}C-MET and ^{11}C-4DST detected positive lesions, whereas ^{18}F-FDG detected an equivocal lesion. ^{18}F-FDG was rarely able to detect skull lesions because of the high physiological accumulation in the brain, whereas ^{11}C-MET and ^{11}C-4DST were capable of clearly detecting skull lesions because of their low accumulation in the brain. Furthermore, ^{11}C-4DST and ^{11}C-MET had higher diagnostic accuracies than that of ^{18}F-FDG, when compared with iliac crest biopsy. However, no significant difference was observed between the ^{11}C-MET and ^{11}C-4DST findings.

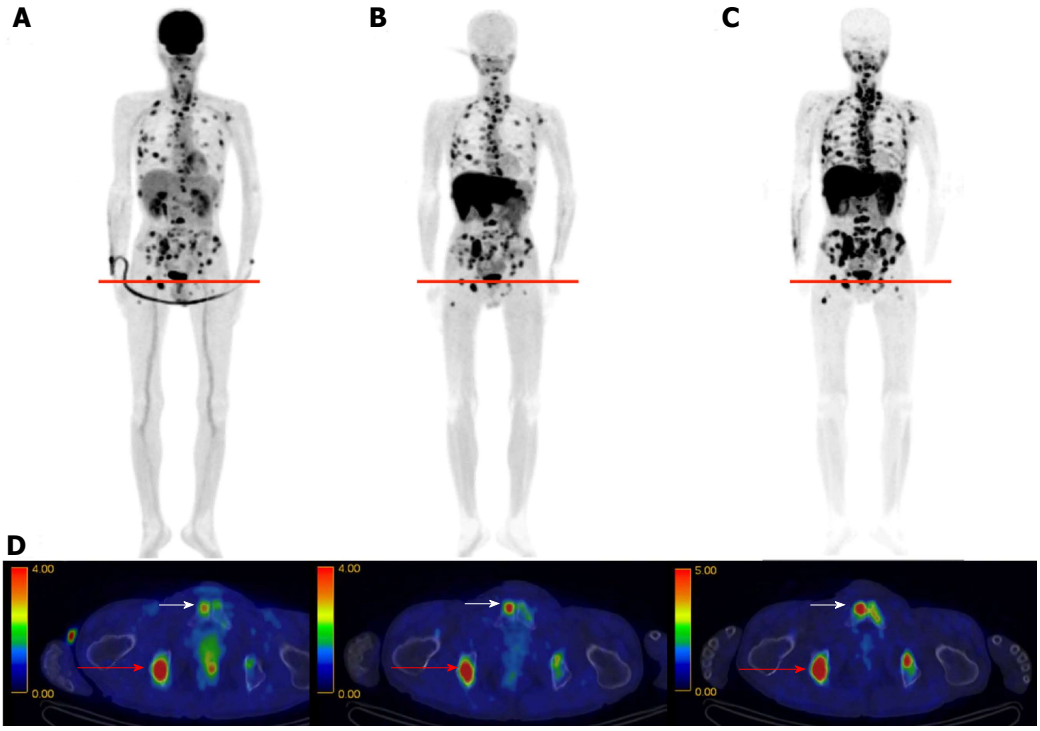

Figure 9 4'-[methyl-^{11}C]-thiothymidine images in multiple myeloma. ^{18}F-FDG (A), ^{11}C-MET (B), and ^{11}C-4DST (C) PET images obtained in a 63-year-old man with multiple myeloma. Numerous active lesions are visible in the three maximum intensity projection images. The fusion images are for the cross-section at the level indicated by the red lines (D). The lesion in the right ischium (red arrow) was positive in all three PET scans. However, the lesion in the right pubis (white arrow) was only positive on the ^{11}C-MET and ^{11}C-4DST PET scans and was equivocal on the ^{18}F-FDG PET scan. Reprinted from Okasaki *et al*[24], with the permission of Springer. ^{11}C-4DST: 4'-[methyl-^{11}C]-thiothymidine; ^{11}C-MET: ^{11}C-Methionine; ^{18}F-FDG: 2-Deoxy-2-[^{18}F]fluoro-D-glucose; PET: Positron emission tomography.

RENAL CELL CANCER

Minamimoto *et al*[25] evaluated the potential of ^{11}C-4DST PET/CT for imaging cellular proliferation in advanced clear cell renal cell cancer (RCC), compared with ^{18}F-FDG PET/CT[25]. Five patients with a single RCC lesion were examined. The typical tumor accumulation pattern of ^{18}F-FDG was diffuse or with a thick uptake layer, in contrast to outer surface-dominant uptake with ^{11}C-4DST (Figure 10). The SUVmax of ^{11}C-4DST (7.3 ± 12.2) was slightly higher than that of ^{18}F-FDG (6.0 ± 12.8). The correlation between SUVmax and Ki-67 index was higher with ^{11}C-4DST (r = 0.61) than with ^{18}F-FDG (r = 0.43). Tumor uptake of both tracers was correlated with the Fuhrman nuclear grading system. Interestingly, the ^{11}C-4DST uptake increased as the degree of pathological phosphorylation of mammalian target of rapamycin (pmTOR) increased. This might indicate that ^{11}C-4DST has potential for use in evaluating the therapeutic effect of mTOR inhibitors in patients with RCC.

4DST IN BASIC RESEARCH

In cancer, differential diagnosis of benign *vs* malignant lesions is important. Toyohara *et al*[26] investigated whether 4DST is useful for differentially diagnosing tumors and inflammation in animal models[26]. C6 glioma cells were transplanted into the right shoulder of Wistar rats, and turpentine was injected into the left hind leg 9 d later to create a tumor and acute inflammation model. Dynamic ^{11}C-4DST PET scan was performed one day after turpentine injection. The biodistribution of ^{11}C-4DST was determined and compared with those of ^{18}F-FLT, ^{18}F-FDG, ^{11}C-choline, ^{11}C-MET, and two sigma receptor ligands 1-4-2'-^{18}F-fluoroethoxy-3-methoxyphenethyl-4-3-4-fluorophenyl-propyl-piperazine (^{18}F-FE-SA5845) and 1-3,4-^{11}C-dimethoxyphenylethyl-4-3-phenylpropyl-piperazine (^{11}C-SA4503). The results showed that ^{11}C-4DST had the highest tumor uptake among the tracers examined (SUV = 4.9), and the tumor muscle ratio was 13, which is equivalent to that of ^{18}F-FDG. ^{11}C-4DST showed an extremely high tumor inflammation ratio of 49, which was comparable to that of ^{18}F-FE-SA5845, and was more than 10-fold higher than that of ^{18}F-FDG. ^{11}C-4DST showed a persistent increase in accumulation in the tumor and bone marrow. On the other hand, it was not retained in inflammatory tissues, and returned to the same level as in muscles 40 min after injection. As indicated here, ^{11}C-4DST is a useful PET tracer with high sensitivity and specificity, with completely different dynamics in tumors and inflammatory tissue. The above results strongly suggest that ^{11}C-4DST will be effective in clinical settings.

In a follow-up study, Toyohara *et al*[27] evaluated longitudinal changes in ^{11}C-4DST uptake in turpentine-induced acute, subacute, and chronic phases of inflammatory tissues[27]. They found that ^{11}C-4DST uptake in inflammatory tissue was transiently increased during the subacute phase and subsequently decreased to normal levels. The transient increase in ^{11}C-4DST

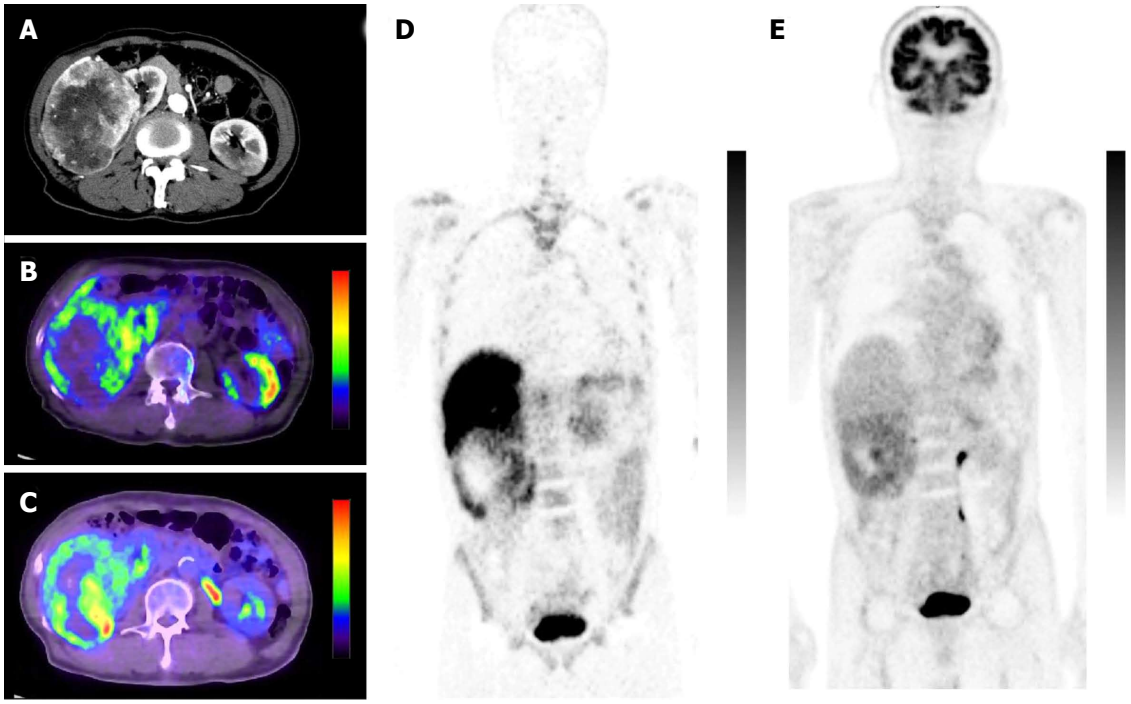

Figure 10 4'-[methyl-^{11}C]-thiothymidine images in clear cell renal carcinoma. A 78-year-old male with a clear cell renal carcinoma (RCC) in the right kidney. Contrast-enhanced abdominal CT (A), fused ^{11}C-4DST PET/CT (axial image) (B), fused ^{18}F-FDG PET/CT (axial image) (C), coronal ^{11}C-4DST PET (D), and coronal ^{18}F-FDG PET (E) images are shown. The uptake of ^{11}C-4DST was predominantly near the outer surface of the RCC tumor; the uptake of ^{18}F-FDG was more diffuse. Reprinted from Minamimoto *et al*[25], with the permission of Springer. ^{11}C-4DST: 4'-[methyl-^{11}C]-thiothymidine; ^{18}F-FDG: 2-Deoxy-2-[^{18}F]fluoro-D-glucose; PET: Positron emission tomography; CT: Computed tomography.

uptake paralleled changes in the Ki-67 labeling index in inflammatory tissues. These data indicate that avoiding the subacute phase is required for proper evaluation of tumor responses using ^{11}C-4DST PET.

Tsuji *et al*[28] established a clinically relevant mouse model of mesothelioma[28] and applied ^{11}C-4DST as a tool to differentiate histological subtypes. In their mouse model, ^{11}C-4DST was suitable for imaging the epithelioid subtype, while ^{18}F-FDG was more suitable for the sarcomatoid subtype.

Hasegawa *et al*[29] evaluated radiation induced carcinogenesis and its suppression by ^{11}C-4DST PET in a radiation-induced thymic lymphoma model[29]. They found initial higher ^{11}C-4DST uptake in irradiated thymus at 1 wk after fractionated whole-body X-ray irradiation. The increased ^{11}C-4DST uptake in the thymus was completely abolished by bone marrow transplantation. This study demonstrates the feasibility of cellular proliferation imaging with ^{11}C-4DST for the noninvasive monitoring of tumorigenic processes in animal models of radiation-induced cancer.

CONCLUSION

^{11}C-4DST is a newly developed PET tracer that can be used to image DNA synthesis, and its application in clinical settings is being studied at several facilities. In the future, ^{11}C-4DST will be applied to more types of cancer, which will further establish the significance of ^{11}C-4DST PET diagnoses through the accumulation of data on the physiological accumulation in lesions.

ACKNOWLEDGMENTS

The author thanks Mr. Kunpei Hayashi for the production of ^{11}C-4DST. Figures 4, 6 and 7 were reprinted from Nariai *et al*[14], with the permission of Springer. Figures 3 and 8 were reprinted from Toyohara *et al*[10] and Minamimoto *et al*[22], respectively, with the permission of the Society of Nuclear Medicine and Molecular Imaging, Inc. Figures 9 and 10 were reprinted from Okasaki *et al*[24] and Minamimoto *et al*[25], respectively, with the permission of Springer.

REFERENCES

1 **Bading JR**, Shields AF. Imaging of cell proliferation: status and prospects. *J Nucl Med* 2008; **49** Suppl 2: 64S-80S [PMID: 18523066 DOI: 10.2967/jnumed.107.046391]

2 **Toyohara J**, Fujibayashi Y. Trends in nucleoside tracers for PET imaging of cell proliferation. *Nucl Med Biol* 2003; **30**: 681-685 [PMID: 14499325 DOI: 10.1016/S0969-8051(03)00084-2]

3 **Christman D**, Crawford EJ, Friedkin M, Wolf AP. Detection of DNA synthesis in intact organisms with positron-emitting (methyl-11 C)thymidine. *Proc Natl Acad Sci USA* 1972; **69**: 988-992 [PMID: 4554538 DOI: 10.1073/pnas.69.4.988]

4 **Mankoff DA**, Shields AF, Graham MM, Link JM, Eary JF, Krohn KA. Kinetic analysis of 2-[carbon-11]thymidine PET imaging studies: compartmental model and mathematical analysis. *J Nucl Med* 1998; **39**: 1043-1055 [PMID: 9627342]

5 **Mankoff DA**, Shields AF, Link JM, Graham MM, Muzi M, Peterson LM, Eary JF, Krohn KA. Kinetic analysis of 2-[11C]thymidine PET imaging studies: validation studies. *J Nucl Med* 1999; **40**: 614-624

[PMID: 10210220]
6 **Wells JM**, Mankoff DA, Eary JF, Spence AM, Muzi M, O'Sullivan F, Vernon CB, Link JM, Krohn KA. Kinetic analysis of 2-[11C]thymidine PET imaging studies of malignant brain tumors: preliminary patient results. *Mol Imaging* 2002; **1**: 145-150 [PMID: 12920852 DOI: 10.1162/153535002760235445]
7 **Wells JM**, Mankoff DA, Muzi M, O'Sullivan F, Eary JF, Spence AM, Krohn KA. Kinetic analysis of 2-[11C]thymidine PET imaging studies of malignant brain tumors: compartmental model investigation and mathematical analysis. *Mol Imaging* 2002; **1**: 151-159 [PMID: 12920853 DOI: 10.1162/153535002760235454]
8 **Toyohara J**, Kumata K, Fukushi K, Irie T, Suzuki K. Evaluation of 4'-[methyl-14C]thiothymidine for in vivo DNA synthesis imaging. *J Nucl Med* 2006; **47**: 1717-1722 [PMID: 17015909]
9 **Toyohara J**, Okada M, Toramatsu C, Suzuki K, Irie T. Feasibility studies of 4'-[methyl-(11)C]thiothymidine as a tumor proliferation imaging agent in mice. *Nucl Med Biol* 2008; **35**: 67-74 [PMID: 18158945 DOI: 10.1016/j.nucmedbio.2007.10.001]
10 **Toyohara J**, Nariai T, Sakata M, Oda K, Ishii K, Kawabe T, Irie T, Saga T, Kubota K, Ishiwata K. Whole-body distribution and brain tumor imaging with (11)C-4DST: a pilot study. *J Nucl Med* 2011; **52**: 1322-1328 [PMID: 21764794 DOI: 10.2967/jnumed.111.088435]
11 **Koyama H**, Siqin Z, Sumi K, Hatta Y, Nagata H, Doi H, Suzuki M. Highly efficient syntheses of [methyl-11C]thymidine and its analogue 4'-[methyl-11C]thiothymidine as nucleoside PET probes for cancer cell proliferation by Pd(0)-mediated rapid C-[11C]methylation. *Org Biomol Chem* 2011; **9**: 4287-4294 [PMID: 21503302 DOI: 10.1039/c0ob01249a]
12 **Zhang Z**, Doi H, Koyama H, Watanabe Y, Suzuki M. Efficient syntheses of [^{11}C]zidovudine and its analogs by convenient one-pot palladium(0)-copper(I) co-mediated rapid C-[^{11}C]methylation. *J Labelled Comp Radiopharm* 2014; **57**: 540-549 [PMID: 24992010 DOI: 10.1002/jlcr.3213]
13 **Plotnik DA**, Wu S, Linn GR, Yip FC, Comandante NL, Krohn KA, Toyohara J, Schwartz JL. In vitro analysis of transport and metabolism of 4'-thiothymidine in human tumor cells. *Nucl Med Biol* 2015; **42**: 470-474 [PMID: 25659855 DOI: 10.1016/j.nucmedbio.2014.12.005]
14 **Nariai T**, Inaji M, Sakata M, Toyohara J. Use of 11C-4DST-PET for imaging human brain tumors. In: Hayat MA. Tumors of the Central Nervous System, Volume 11. Netherlands: Springer, 2014: 41-48 [DOI: 10.1007/978-94-007-7037-9_3]
15 **Toyota Y**, Miyake K, Kawai N, Hatakeyama T, Yamamoto Y, Toyohara J, Nishiyama Y, Tamiya T. Comparison of 4'-[methyl-(11)C]thiothymidine ((11)C-4DST) and 3'-deoxy-3'-[(18)F]fluorothymidine ((18)F-FLT) PET/CT in human brain glioma imaging. *EJNMMI Res* 2015; **5**: 7 [PMID: 25853013 DOI: 10.1186/s13550-015-0085-3]
16 **Tanaka K**, Yamamoto Y, Maeda Y, Yamamoto H, Kudomi N, Kawai N, Toyohara J, Nishiyama Y. Correlation of 4'-[methyl-(11)C]-thiothymidine uptake with Ki-67 immunohistochemistry and tumor grade in patients with newly diagnosed gliomas in comparison with (11)C-methionine uptake. *Ann Nucl Med* 2016; **30**: 89-96 [PMID: 26511019 DOI: 10.1007/s12149-015-1035-x]
17 **Ito K**, Yokoyama J, Miyata Y, Toyohara J, Okasaki M, Minamimoto R, Morooka M, Ishiwata K, Kubota K. Volumetric comparison of positron emission tomography/computed tomography using 4'-[methyl-^{11}C]-thiothymidine with 2-deoxy-2-^{18}F-fluoro-D-glucose in patients with advanced head and neck squamous cell carcinoma. *Nucl Med Commun* 2015; **36**: 219-225 [PMID: 25369751 DOI: 10.1097/MNM.0000000000000241]
18 **Koyasu S**, Nakamoto Y, Kikuchi M, Suzuki K, Hayashida K, Itoh K, Togashi K. Prognostic value of pretreatment 18F-FDG PET/CT parameters including visual evaluation in patients with head and neck squamous cell carcinoma. *AJR Am J Roentgenol* 2014; **202**: 851-858 [PMID: 24660716 DOI: 10.2214/AJR.13.11013]
19 **Lim R**, Eaton A, Lee NY, Setton J, Ohri N, Rao S, Wong R, Fury M, Schöder H. 18F-FDG PET/CT metabolic tumor volume and total lesion glycolysis predict outcome in oropharyngeal squamous cell carcinoma. *J Nucl Med* 2012; **53**: 1506-1513 [PMID: 22895812 DOI: 10.2967/jnumed.111.101402]
20 **Dibble EH**, Alvarez AC, Truong MT, Mercier G, Cook EF, Subramaniam RM. 18F-FDG metabolic tumor volume and total glycolytic activity of oral cavity and oropharyngeal squamous cell cancer: adding value to clinical staging. *J Nucl Med* 2012; **53**: 709-715 [PMID: 22492732 DOI: 10.2967/jnumed.111.099531]
21 **Moon SH**, Choi JY, Lee HJ, Son YI, Baek CH, Ahn YC, Park K, Lee KH, Kim BT. Prognostic value of 18F-FDG PET/CT in patients with squamous cell carcinoma of the tonsil: comparisons of volume-based metabolic parameters. *Head Neck* 2013; **35**: 15-22 [PMID: 22307893 DOI: 10.1002/hed.22904]
22 **Minamimoto R**, Toyohara J, Seike A, Ito H, Endo H, Morooka M, Nakajima K, Mitsumoto T, Ito K, Okasaki M, Ishiwata K, Kubota K. 4'-[Methyl-11C]-thiothymidine PET/CT for proliferation imaging in non-small cell lung cancer. *J Nucl Med* 2012; **53**: 199-206 [PMID: 22190643 DOI: 10.2967/jnumed.111.095539]
23 **Minamimoto R**, Toyohara J, Ito H, Seike A, Miyata Y, Morooka M, Okasaki M, Nakajima K, Ito K, Ishiwata K, Kubota K. A pilot study of 4'-[methyl-11C]-thiothymidine PET/CT for detection of regional lymph node metastasis in non-small cell lung cancer. *EJNMMI Res* 2014; **4**: 10 [PMID: 24593883 DOI: 10.1186/2191-219X-4-10]
24 **Okasaki M**, Kubota K, Minamimoto R, Miyata Y, Morooka M, Ito K, Ishiwata K, Toyohara J, Inoue T, Hirai R, Hagiwara S, Miwa A. Comparison of (11)C-4'-thiothymidine, (11)C-methionine, and (18)F-FDG PET/CT for the detection of active lesions of multiple myeloma. *Ann Nucl Med* 2015; **29**: 224-232 [PMID: 25421383 DOI: 10.1007/s12149-014-0931-9]
25 **Minamimoto R**, Nakaigawa N, Nagashima Y, Toyohara J, Ueno D, Namura K, Nakajima K, Yao M, Kubota K. Comparison of 11C-4DST and 18F-FDG PET/CT imaging for advanced renal cell carcinoma: preliminary study. *Abdom Radiol* (NY) 2016; **41**: 521-530 [PMID: 27039323 DOI: 10.1007/s00261-015-0601-y]
26 **Toyohara J**, Elsinga PH, Ishiwata K, Sijbesma JW, Dierckx RA, van Waarde A. Evaluation of 4'-[methyl-11C]thiothymidine in a rodent tumor and inflammation model. *J Nucl Med* 2012; **53**: 488-494 [PMID: 22315439 DOI: 10.2967/jnumed.111.098426]
27 **Toyohara J**, Sakata M, Oda K, Ishii K, Ishiwata K. Longitudinal observation of [11C]4DST uptake in turpentine-induced inflammatory tissue. *Nucl Med Biol* 2013; **40**: 240-244 [PMID: 23141551 DOI: 10.1016/j.nucmedbio.2012.10.008]
28 **Tsuji AB**, Sogawa C, Sugyo A, Sudo H, Toyohara J, Koizumi M, Abe M, Hino O, Harada YN, Furukawa T, Suzuki K, Saga T. Comparison of conventional and novel PET tracers for imaging mesothelioma in nude mice with subcutaneous and intrapleural xenografts. *Nucl Med Biol* 2009; **36**: 379-388 [PMID: 19423005 DOI: 10.1016/j.nucmedbio.2009.01.018]
29 **Hasegawa S**, Morokoshi Y, Tsuji AB, Kokubo T, Aoki I, Furukawa T, Zhang MR, Saga T. Quantifying initial cellular events of mouse radiation lymphomagenesis and its tumor prevention in vivo by positron emission tomography and magnetic resonance imaging. *Mol Oncol* 2015; **9**: 740-748 [PMID: 25510653 DOI: 10.1016/j.molonc.2014.11.009]
30 **Lu L**, Bergström M, Fasth KJ, Langström B. Synthesis of [76Br]bromofluorodeoxyuridine and its validation with regard to uptake, DNA incorporation, and excretion modulation in rats. *J Nucl Med* 2000; **41**: 1746-1752 [PMID: 11038007]

P- Reviewer: Chow J, Gao BL **S- Editor**: Qiu S
L- Editor: Wang TQ **E- Editor**: Wu HL

Published by **Baishideng Publishing Group Inc**
8226 Regency Drive, Pleasanton, CA 94588, USA
Telephone: +1-925-223-8242
Fax: +1-925-223-8243
E-mail: bpgoffice@wjgnet.com
Help Desk: http://www.wjgnet.com/esps/helpdesk.aspx
http://www.wjgnet.com